

Chemistry of Convex *versus* Concave Carbon: The Reactive Exterior and the Inert Interior of C₆₀

Harald Mauser¹, Andreas Hirsch^{1*}, Nicolaas J.R. van Eikema Hommes², and Timothy Clark^{2,*}

¹Institut für Organische Chemie, Universität Erlangen-Nürnberg, Henkestraße 42, D-91054 Erlangen, Germany; Fax: +49-9131-85-6864 (hirsch@organik.uni-erlangen.de)

²Computer-Chemie-Centrum, Institut für Organische Chemie, Universität Erlangen-Nürnberg, Nägelsbachstr. 25, D-91052 Erlangen, Germany; Fax: +49-9131-85-6565 (clark@organik.uni-erlangen.de)

Received: 2 September 1997 / Accepted: 18 September 1997 / Published: 15 October 1997

Abstract

Do the chemical properties of the surface of a carbon sheet depend on its shape? This question addresses a criterion for chemical behaviour that has hardly been investigated previously. The current neglect of this question may be due to the fact that suitable model systems with easily distinguishable graphitic surfaces were essentially unknown until the discovery [1] and synthesis [2,3,4] of fullerenes, nanotubes and other related forms of carbon. In this study, we present the first systematic comparison of the chemical behaviour of the convex outer and the concave inner surfaces of C₆₀ by analysing the results of semiempirical and DFT calculations on exohedral and endohedral complexes with H- and F-atoms as well as with the methyl radical. We show that such extremely reactive species are trapped by the extraordinary inert inner surface of C₆₀ and do not undergo chemical reactions.

Keywords: Fullerene, Semiempirical calculation, DFT calculation, Endohedral complexes

Introduction

The spherical structure of fullerenes [1-4] allows exohedral and endohedral chemistries to be distinguished. Especially, the covalent exohedral chemistry of C₆₀ has been well established over the last few years and principles of the behaviour of C₆₀ towards external addition reactions can be deduced [5]. For this type of chemistry, the fullerenes are certainly more reactive than planar aromatics because the driving force for such addition reactions is the reduction of strain [6], which

results from pyramidalization in the sp²-carbon network. Two types of endohedral derivatives [7] are well known, the inclusion compounds of electropositive metals and those of noble gases. In the former systems, a cation is encapsulated by a negatively charged carbon shell, whereas in the latter both components are neutral. Endohedral derivatives involving covalent bonds between the guest and the inner surface are unknown. Several theoretical calculations concerning the stability, geometry and electronic structures of covalent exohedral [5] derivatives as well as of fullerenes [7] encapsulating non covalently bound cations, anions and neutrals

* To whom correspondence should be addressed

Table 1. Comparison between DFT and semiempirical results for the system F/C₆₀

Compound		PM3			UB3LYP/D95*/PM3		rel. Energy (kcal/mol)
		Coulson Charge [a]	ΔH_f^0 (kcal/mol)	$\delta\Delta H_f^0$ (kcal/mol)	Mulliken Charge [b]	total Energy (- a.u.)	
FC ₆₀ (<i>exo</i>)		-0.10	749.20	-68.82	-0.16	2386.18979	-56.7
F@C ₆₀ (<i>endo</i>)	bound	-0.22	838.56	20.54	-0.30	2386.09185	4.8
	transition state	-0.38	848.50	30.48	-0.45	2386.11069	-7.9
	centre	0.00	827.25	9.23	-0.53	2386.13948	-25.1

[a] charge for the F-atom.

[b] charge for the F-atom.

are available but so far no investigations have addressed the introductory question.

Computational Method

All semiempirical calculations in this study used the VAMP 6.1 [8] program with the PM3 [9] Hamiltonian within the unrestricted Hartree-Fock (UHF) formalism and the DFT calculations were performed with the UB3LYP/D95* Method [10] in Gaussian 94 [11] using the PM3 geometry. Although

Table 2. PM3 dipole moments, Coulson charges, heats of formation and bond energies of exohedral and endohedral complexes of C₆₀ with H, F and the methyl radical (Me).

Compound		Dipole-moment (Debye)	Coulson Charge [a]	HF (kcal/mol)	Bond Energy (kcal/mol)
HC ₆₀ (<i>exo</i>)		1.22	0.12	783.29	-67.97
H@C ₆₀ (<i>endo</i>)	bound	0.51	0.05	851.21	-0.05
	transition state	0.16	-0.04	855.95	4.69
	unbound minimum	0.07	-0.02	848.89	-2.37
FC ₆₀ (<i>exo</i>)		1.23	-0.10	749.20	-68.82
F@C ₆₀ (<i>endo</i>)	bound	0.25	-0.22	838.56	20.54
	transition state	1.13	-0.38	848.50	30.48
	centre	0.00	0.00	827.25	9.23
CH ₃ C ₆₀ (<i>exo</i>)		1.48	0.08	778.78	-48.34
CH ₃ @C ₆₀ (<i>endo</i>)	bound	0.31	-0.05	885.08	57.96
	transition state	0.25	-0.08	886.15	59.03
	centre	0.00	-0.02	839.17	12.05

[a] of H, F and Me

the numerical value of the UHF $\langle S^2 \rangle$ is very high for fullerene/radical adducts [12] (and also for C₆₀ itself), the energetic and geometric effects of spin-contamination are small because of the very high multiplicities of the principal spin contaminants.

Results and Discussion

The reaction profile shown in Figure 1 and Table 1 stresses the very different reactivity of fluorine inside and outside the fullerene cage. The energy curve of the methyl complexes is qualitatively the same. The exohedral addition of fluorine is a very exothermic reaction, resulting in bound structure (D). Moving inside C₆₀, the addition of fluorine is now endothermic for the bound F@C₆₀ (C). After passing a transition state (B), fluorine reaches the endohedral minimum (A) in the centre of C₆₀ at a distance of 3.56 Å to the C-atoms of the cage. According to the B3LYP result the PM3 transition state

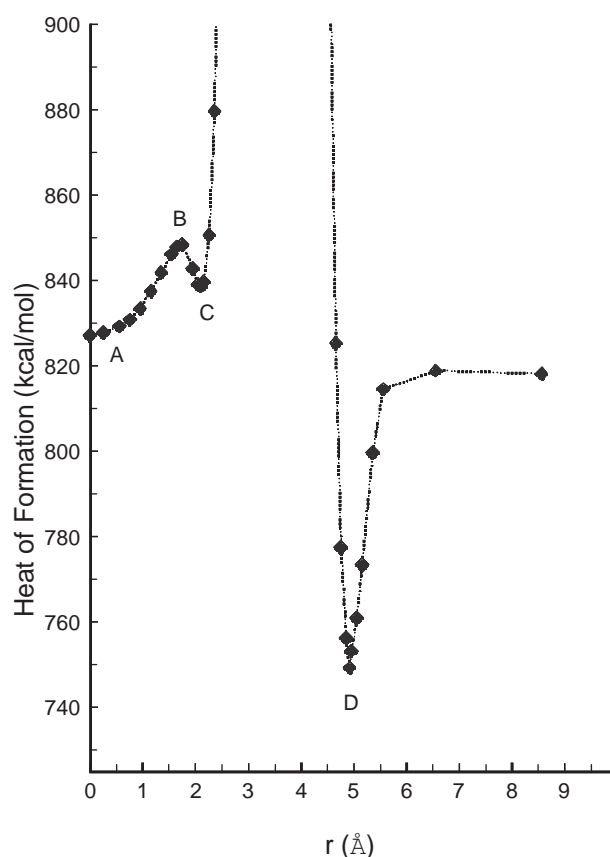


Figure 1. PM3-UHF heats of formation of fluorine C_{60} complexes as a function of the F/cage-centre distance r . The reaction coordinate describes the movement of an F-atom from the cage centre towards a C-atom. The extrema $F@C_{60}$ (centre) (A), $F@C_{60}$ (transition state of endo addition) (B), $F@C_{60}$ (bound) (C), FC_{60} (exo) (D) of this reaction coordinate represent fully geometry- optimised structures.

is lower in energy than the bound structure, which indicates a very low dissociation barrier, if any.

Further computational results are shown in Tables 2 and 3. Figure 2 shows the PM3-structures of $F@C_{60}$, which are representative for the corresponding structures for $H@C_{60}$ and $Me@C_{60}$ (A-D in Figure 1). The exact geometries are shown for the pyracylene subunits of $F@C_{60}$ (Figure 3), which are comparable to those of $H@C_{60}$ and $Me@C_{60}$ (Table 3). These results can be summarised as follows:

1) The covalent exohedral derivatives FC_{60} , HC_{60} and MeC_{60} are considerably more stable than the endohedrals $F@C_{60}$, $H@C_{60}$ and $Me@C_{60}$, regardless of the bonding situation within the cage.

2) The most favourable encapsulations of F and Me by C_{60} are slightly endothermic, whereas that of H is slightly exothermic at the PM3 level of calculation. The encapsulation of F is 25 kcal/mol exothermic at UB3LYP/D95*/PM3.

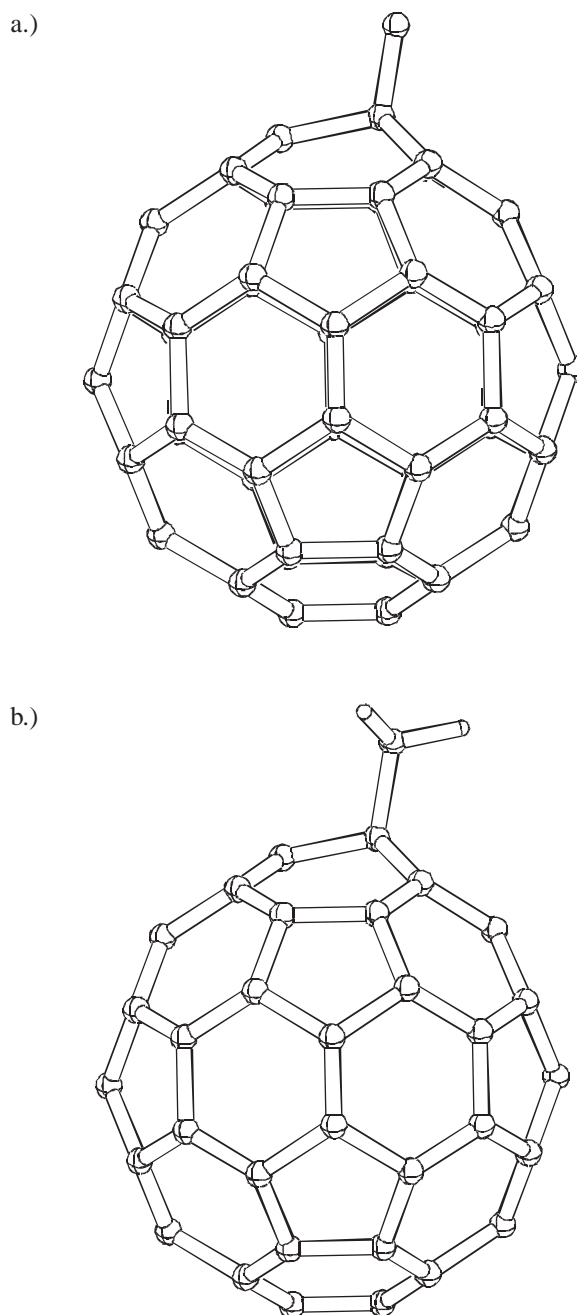


Figure 2a-b. PM3-UHF-geometries of a) FC_{60} (exo), b) CH_3C_{60} (exo)

3) The structures of $F@C_{60}$ and $Me@C_{60}$ with the guests placed exactly in the centre of the cage [15] are the most stable endohedral structures. In case of $H@C_{60}$, we observe a slightly different behaviour. Hydrogen is quite free inside C_{60} and barriers between the bound and the endohedral minimum structure of $H@C_{60}$ are very low (Table 2). The exact location of the endohedral minimum of $H@C_{60}$ depends on the method of calculation, but it is consistently slightly off-centre (1.1 Å from the centre with the PM3-Hamiltonian).

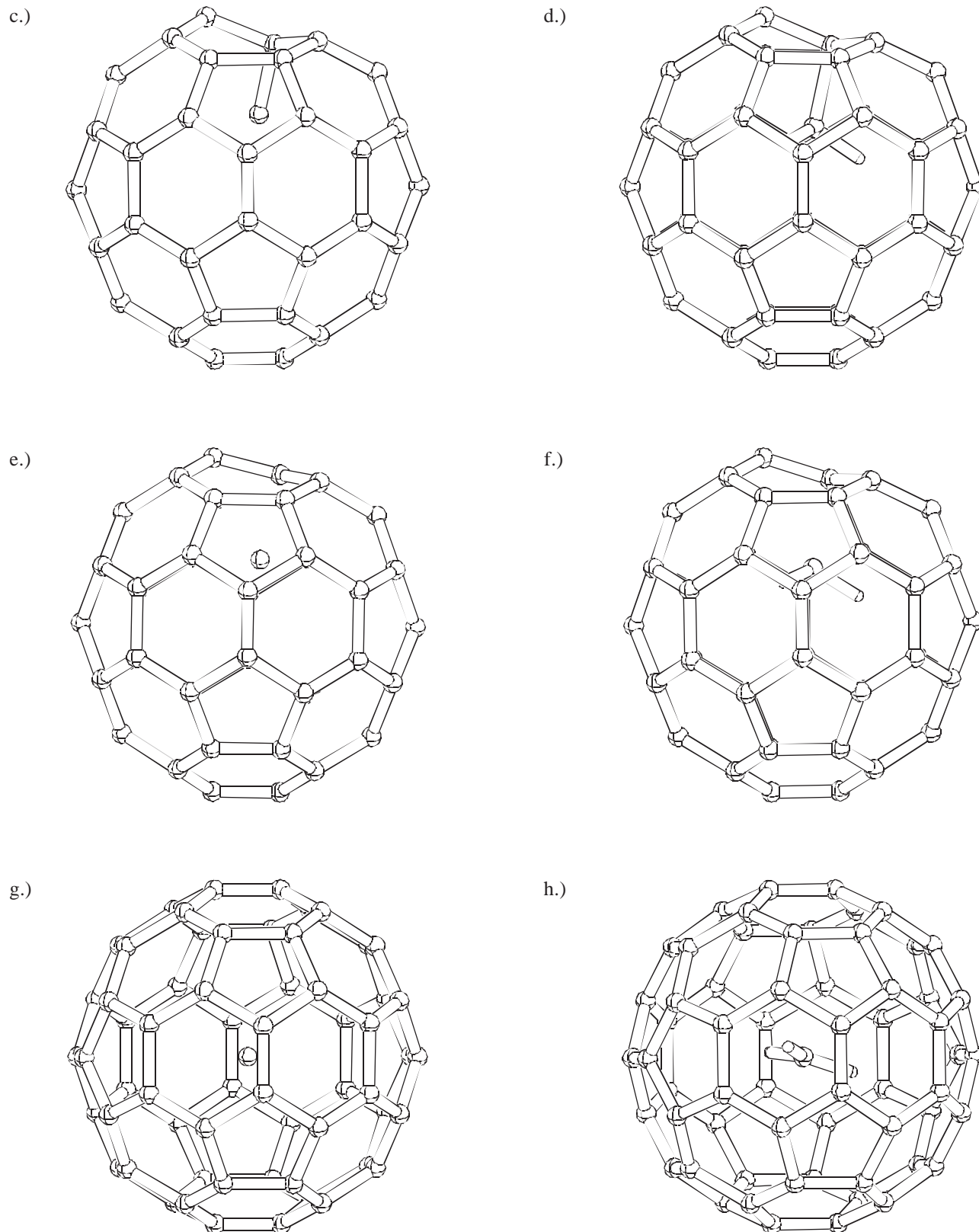


Figure 2c-h. PM3-UHF-geometries of c) $F@C_{60}$ (bound), d) $CH_3@C_{60}$ (bound), e) $F@C_{60}$ (transition state of endo addition), f) $CH_3@C_{60}$ (transition state of endo addition), g) $F@C_{60}$ (centre), h) $CH_3@C_{60}$ (centre).

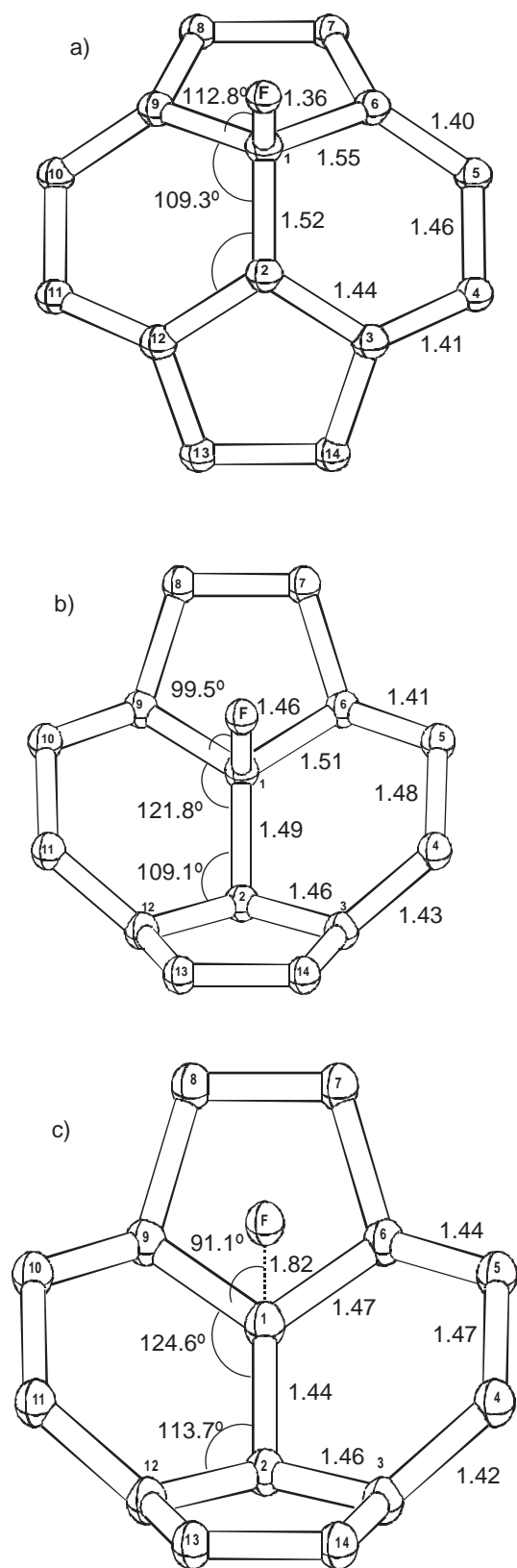


Figure 3. Selected bond lengths and bond angles of a) FC_{60} (exo) b) $F@C_{60}$ (bound) and c) $F@C_{60}$ (transition state of endo addition). For clarity only the neighbouring pyracylene units are shown.

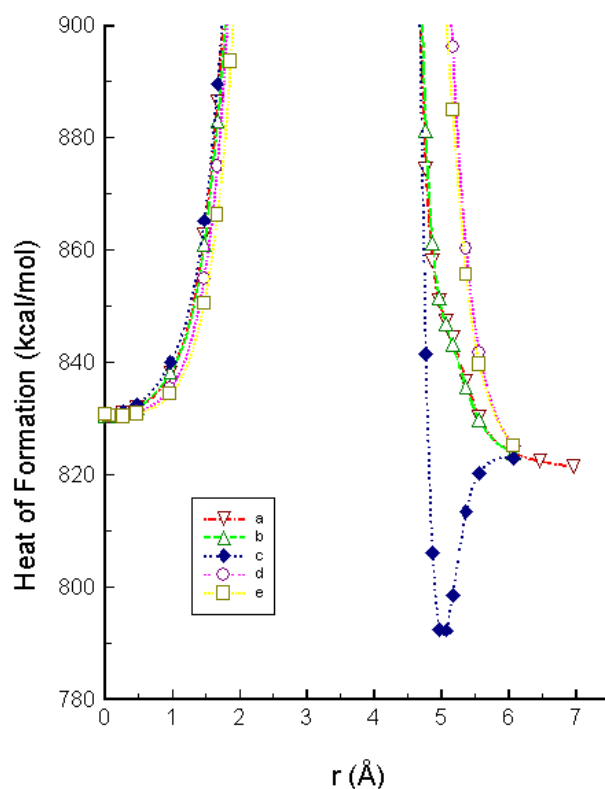


Figure 4. Calculated PM3-UHF heats of formation of fluorine C_{60} complexes (single points energies involving the undistorted fullerene cage) as a function of the F/cage centre distance r . The displacement directions are the cage-centre to (a) the centre of a [5,6]-bond, (b) the centre of a [6,6]-bond, (c) a C-atom, (d) the centre of a pentagon and (e) the centre of a hexagon.

4) In contrast to endohedral complexes of C_{60} with electropositive metals [7], no charge-transfer occurs between the guest and the host in the global minimum structures of $H@C_{60}$ and $Me@C_{60}$. In the case of $F@C_{60}$ according to DFT-calculation (B3LYP/D95*/PM3) there is a partial negative charge on the encapsulated fluorine (Table 1).

5) Only local minima are found for those isomers of $H@C_{60}$, $F@C_{60}$ and $Me@C_{60}$ where the guest is covalently bound to a C-atom (Table 2, Figure 1).

6) The covalent binding of H, F or Me with the inner surface of C_{60} leads to a very unfavourable cage distortion (Table 3, Figure 3). This is especially reflected e.g. by the bond angles $C_9C_1C_2$, which differ strongly from the ideal tetrahedral geometry and by the unusually long 'single' bonds between the guests and the host. The corresponding values of the exohedral adducts are those of normal strain free arrangements around sp^3 -C-atoms.

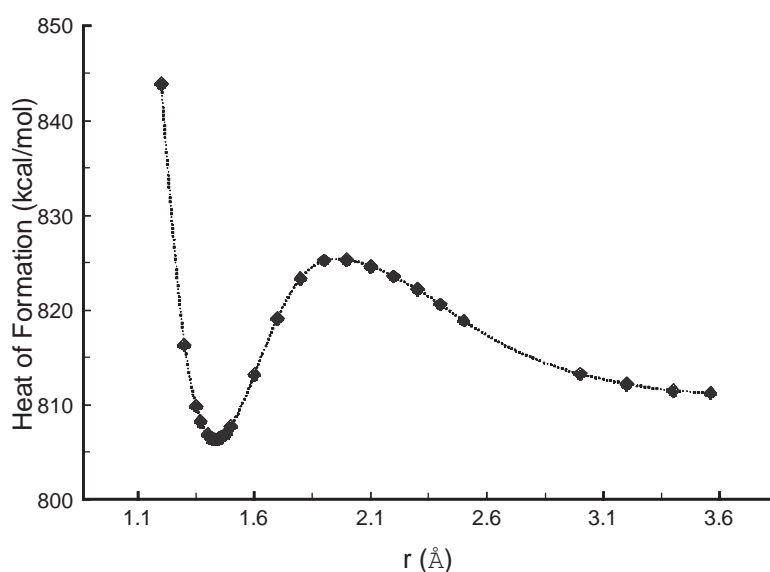
We interpret these results as follows: The predominant driving force for exohedral addition reactions is the relief of strain energy [5,6,14]. The pyramidalization of the C-atoms within the fullerenes is driven by the geometrical constraints

Table 3. Selected bond lengths and bond angles of exohedral and endohedral complexes of H, F and Me with C₆₀

Compound		C-E bond lengths		Bond angles (deg.)	
			(Å)	C ₉ C ₁ C ₂	C ₉ C ₁ E
C ₆₀			–	120.0	–
HC ₆₀ (exo)			1.12	110.7	112.1
H@C ₆₀ (endo)	bound		1.17	125.2	92.4
	transition state		1.43	124.9	86.9
FC ₆₀ (exo)			1.36	109.3	112.8
F@C ₆₀ (endo)	bound		1.46	121.8	99.5
	transition state		1.82	109.3	91.1
CH ₃ C ₆₀ (exo)			1.52	109.7	112.7
CH ₃ @C ₆₀ (endo)	bound		1.68	121.1	99.8
	transition state		1.87	123.5	95.3

of the σ -system. The conjugated C-atoms of a fullerene respond to the deviation from planarity by rehybridization of the sp^2 σ and p π orbitals, since pure p character of π orbitals is only possible in strictly planar situations. The electronic structure of non planar conjugated organic molecules has been discussed by Haddon [14] using the π -orbital vector (POAV) analysis. For C₆₀ an average σ -bond hybridization of $sp^{2.278}$ and a π -orbital fractional s character of 0.085 (POAV1) or 0.081 (POAV2) was found [14]. As a consequence, the π -orbitals extend further beyond the outer surface than into the interior of C₆₀, or in other words, the π -electrons are preferably located outside rather than inside the fullerene cage. These geometric and electronic properties of C₆₀ [5,6] are responsible for its very pronounced propensity to undergo

exohedral addition reactions (Table 2, Figure 1), with the formation of covalent bonds involving a newly formed 'strain-free' sp^3 -C-atom within the cage (Table 2, Figure 3). Both the pronounced exposure of the hybrid π -orbitals from the exterior of C₆₀ guaranteeing a favourable orbital overlap with incoming addends (kinetic effect) as well as the strain assistance [6] of the σ -system (thermodynamic effect) facilitate the chemistry of the outer surface. No favourable bonding situation can be achieved by the addition of H, F or Me to a C-atom at the inside of the cage, since instead of relief, additional strain is introduced into the fullerene cage. Apart from this thermodynamic effect, kinetic factors also can be expected to inhibit addition reactions with the inner surface of C₆₀, since the π -orbital extent away from the inner surface is

**Figure 5.** Endohedral addition of the encapsulated F to the inside of the cage after exohedral covalent binding of hydrogen. PM3-UHF heats of formation as a function of the distance r from F to the α -C-atom of F@C₆₀H.

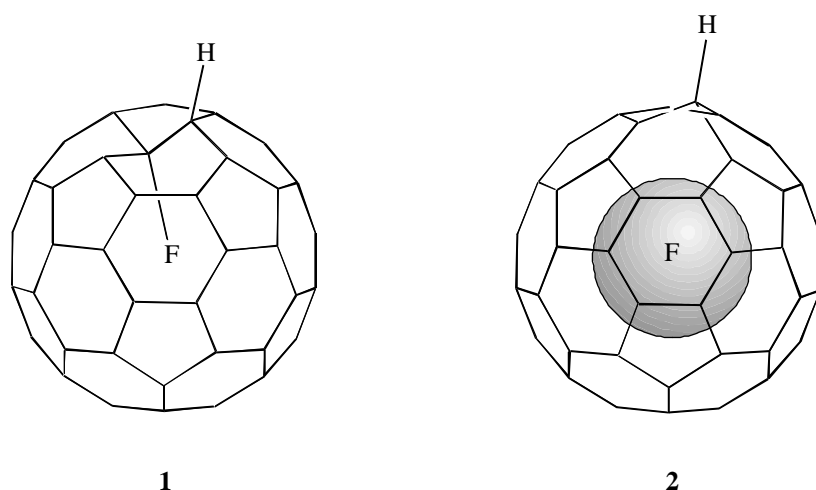


Figure 6. Schematic representation of the compounds of the endohedral addition of the encapsulated F to the inside of the cage after exohedral covalent binding of hydrogen.

considerably smaller than outside the cage, which clearly makes an orbital overlap between a potential addend and a C-atom of the cage much less efficient. Indeed, single point calculations describing the movement of F away from the centre of the cage towards various directions using the undistorted C_{60} -cage indicate that a favourable orbital overlap is only provided if the addend approaches a C-atom from outside the cage (Figure 4). Therefore, when encapsulated by C_{60} , the most favourable situation for such usually extremely reactive species like H- or F-atoms or the methyl radical is to stay in the middle of the cage and to avoid interactions with the inner surface as much as possible. An endohedral addition of the encapsulated radicals is only likely if the fullerene cage is distorted so that the orbital overlap becomes more favourable. This situation can be created by exohedral addition of another radical. Figure 5 shows the energy profile for inside addition of fluorine encapsulated in C_{60} after H was added at the fullerene exterior. The bound structure **1** (Figure 6) is now the global minimum (PM3-UHF: 790.7 kcal/mol) while the isomer **2** (Figure 6) is +20,6 kcal/mol less stable.

Conclusion

We present here for the first time a new aspect of topicity that takes into account the influence of the shape of a bent sheet on its reactivity. We predict that the inner concave surface of C_{60} is inert toward addition reactions, even if extremely reactive neutral guests are encapsulated. This inertness contrasts with the pronounced reactivity of the outer concave surface of C_{60} . This prediction also implies the possibility of studying almost unperturbed atomic species or reactive molecular systems experimentally at ambient conditions once they are encapsulated by the inert inner surface of fullerenes. Recent experimental [15a,b] and theoretical [15c] studies provided the first evidence for the formation and existence a free N-atom as its quartet ground state encapsulated by C_{60} ,

which confirms our prediction. In an upcoming study we will compare the results of such calculations performed for all first row elements and show that the atomic ground state is indeed stabilised by encapsulation in C_{60} . In the light of new developments in fullerene chemistry, where it has already been shown that stable derivatives with holes in the cage [16-20] can be synthesised, it seems to be only a question of time before it will be possible to allow suitable species to penetrate into the interior of a fullerene, reclose the cage and if necessary to perform subsequent modifications like electrochemical electron-transfer reactions in order to synthesise such extraordinary endohedrals like $E@C_{60}$ in pure form and experimentally prove the inertness of the inner surfaces of fullerenes.

Acknowledgement: This work was supported by the BMBF and the Fonds der Chemischen Industrie.

Supplementary material: The XYZ-files for structures shown in Figure 2 are given.

References

1. Kroto, H. W.; Heath, J. R.; O'Brien, S. C.; Curl, R. F.; Smalley, R. E. *Nature* **1985**, *318*, 162.
2. Krätschmer, W.; Lamb, L. D.; Fostiropoulos, K.; Huffman, D. R. *Nature* **1990**, *347*, 354.
3. Iijima, S. *Nature* **1991**, *354*, 56.
4. Ugarte, D. *Nature* **1992**, *359*, 707.
5. For a review see: Hirsch, A. *The Chemistry of the Fullerenes*; Georg Thieme: Stuttgart, 1994.
6. Haddon, R. C. *Science* **1993**, *261*, 1545.
7. For a review see: Bethune, D. S.; Johnson, D. R.; Salem, J. R.; de Vries, M. S.; Yannoni, C. S. *Nature* **1993**, *366*, 123.
8. Rauhut, G.; Alex, A.; Chandrasekhar, J.; Steinke, T.; Sauer, W.; Beck, B.; Hutter, M.; Gedeck, P. and Clark,

- T. *VAMP 6.0*, Oxford Molecular Ltd., Magdalen Centre, Oxford Science Park, Standford-on-Thames, Oxford, OX4 4GA, England, 1996.
9. Stewart, J.J.P. *J. Comput. Chem.* **1989**, *10*, 209; 221.
 10. B3LYP: Stephens, P. J.; Devlin, F. J.; Chabalowski, C. F.; Frisch, M. J. *J. Phys. Chem.* **1994**, *98*, 11623.
 11. Gaussian 94, Revision D.3, Frisch, M. J.; Trucks, G. W.; Schlegel, H. B.; Gill, P. M.; Johnson, B. G.; Robb, M. A.; Cheeseman, J. R.; Keith, T.; Petersson, G. A.; Montgomery, J. A.; Raghavachari, K.; Al-Laham, M. A.; Zakrzewski, V. G.; Ortiz, J. V.; Foresman, J. B.; Cioslowski, J.; Stefanov, B. B.; Nanayakkara, A.; Challacombe, M.; Peng, C. Y.; Ayala, P. Y.; Chen, W.; Wong, M. W.; Andres, J. L.; Replogle, E. S.; Gomberts, R.; Martin, R. L.; Fox, D. J.; Binkley, J. S.; Defrees, D. J.; Baker, J.; Stewart, J. P.; Head-Gordon, M.; Gonzales, C.; Pople, J. A. Gaussian, Inc., Pittsburgh PA **1995**.
 12. Slanina, Z.; Lee, S.-L.; Yu, C.-H. In *Reviews in Computational Chemistry*; Lipkowitz, K. B. and Boyd, D.B. Eds.; VCH: New York, 1996; Vol. 8, pp. 1 - 62.
 13. Erwin, S. E. In *Buckminsterfullerenes*; Billups, E. E.; Ciufolini, M. A. Eds.; VCH: New York, 1993; p. 217.
 14. Haddon, R. C. *Acc. Chem. Res.* **1992**, *25*, 127.
 15. a) Almeida Murphy, T.; Pawlik, T.; Weidinger, A.; Höhne, M.; Alcalá, R.; Spaeth, J. M. *Phys. Rev. Lett.* **1996**, *77*, 1075; b) Knapp, C.; Dinse, K.-P.; Pietzak, B.; Waiblinger, M.; Weidinger, A. *Chem. Phys. Lett.* **1997** in press; c) Mauser, H.; Hommes, N. v. E.; Clark, T.; Hirsch, A.; Pietzak, B.; Weidinger, A.; Dunsch, L. *Angew. Chem.* **1997** in press.
 16. Grösser, T.; Prato, M.; Lucchini, V.; Hirsch, A.; Wudl, F. *Angew. Chem.* **1995**, *107*, 1462; *Angew. Chem. Int. Ed. Engl.* **1995**, *34*, 1343.
 17. Hummelen, J. C.; Prato, M.; Wudl, F. *J. Am. Chem. Soc.* **1995**, *117*, 7003.
 18. Schick, G.; Hirsch, A.; Mauser, H.; Clark, T. *Chem. Eur. J.* **1996**, *2*, 935.
 19. Birkett, P. R.; Avent, A. G.; Darwish, A. D.; Kroto, H. W.; Taylor, R.; Walton, D. R. M. *J. Chem. Soc., Chem. Commun.* **1995**, 1869.
 20. Arce, M.-J.; Viado, A. L.; An, Y.-Z.; Khan, S. I.; Rubin, Y. *J. Am. Chem. Soc.* **1996**, *118*, 3775.